Am J Physiol Heart Circ Physiol 290: H2606–H2613, 2006;
doi:10.1152/ajpheart.01138.2005.

Multiple actions of pifithrin-α on doxorubicin-induced apoptosis in rat myoblastic H9c2 cells

Chu Chang Chua,[1] Xuwan Liu,[2] Jinping Gao,[1] Ronald C. Hamdy,[1] and Balvin H. L. Chua[1]

[1]*Cardiovascular Research Laboratory, James H. Quillen College of Medicine, East Tennessee State University and Veterans Affairs Medical Center, Johnson City, Tennessee; and*

[2]*Department of Pharmacology, University of Pittsburgh, Pittsburgh, Pennsylvania*

Submitted 27 October 2005; accepted in final form 13 January 2006

Chua, Chu Chang, Xuwan Liu, Jinping Gao, Ronald C. Hamdy, and Balvin H. L. Chua. Multiple actions of pifithrin-α on doxorubicin-induced apoptosis in rat myoblastic H9c2 cells. *Am J Physiol Heart Circ Physiol* 290: H2606–H2613, 2006; doi:10.1152/ajpheart.01138.2005.—Doxorubicin (Dox) is a chemotherapeutic agent that causes significant cardiotoxicity. We showed previously that Dox activates p53 and induces apoptosis in mouse hearts. This study was designed to elucidate the molecular events that lead to p53 stabilization, to examine the pathways involved in Dox-induced apoptosis, and to evaluate the effectiveness of pifithrin-α (PFT-α), a p53 inhibitor, in blocking apoptosis of rat H9c2 myoblasts. H9c2 cells that were exposed to 5 μM Dox had elevated levels of p53 and phosphorylated p53 at Ser15. Dox also triggered a transient activation of p38, p42/p44ERK, and p46/p54JNK MAP kinases. Caspase activity assays and Western blot analysis showed that H9c2 cells treated with Dox for 16 h had marked increase in the levels of caspases-2, -3, -8, -9, -12, Fas, and cleaved poly(ADP ribose) polymerase (PARP). There was a concomitant increase in p53 binding activity, cytochrome *c* release, and apoptosis. These results suggest that Dox can trigger intrinsic, extrinsic, and endoplasmic reticulum-associated apoptotic pathways. Pretreatment of cells with PFT-α followed by Dox administration attenuated Dox-induced increases in p53 levels and p53 binding activity and partially blocked the activation of p46/p54JNK and p42/p44ERK. PFT-α also led to decreased levels of caspases-2, -3, -8, -9, -12, Fas, PARP, cytochrome *c* release, and apoptosis. Our results suggest that p53 stabilization is a focal point of Dox-induced apoptosis and that PFT-α interferes with multiple steps of Dox-induced apoptosis.

p53; phosphorylated p53; mitogen-activated protein kinase; caspases

DOXORUBICIN (Dox) is an anthracycline antibiotic that has been widely used for the treatment of acute leukemia, malignant lymphoma, and solid tumors (16, 34, 61). Unfortunately, its effectiveness is limited by its severe cardiotoxicity (21, 45). The prevailing hypothesis for the mechanism of Dox-induced cardiotoxicity includes free radical-mediated lipid peroxidation and alteration of membrane integrity (51, 60). Recent studies suggest that apoptosis plays an important role in Dox-induced cardiotoxicity (1, 8, 20, 54, 65).

Although there are many factors that could mediate apoptosis in Dox-induced cardiotoxicity, we showed in a previous study that Dox-induced apoptosis is at least partially mediated by p53 (32). p53 is a pivotal transcription factor that is involved in cell growth and differentiation (46). In response to stresses such as ionizing radiation, hypoxia, or DNA-damaging agents, p53 mediates cell cycle arrest, DNA repair, or apoptosis to eliminate damaged cells from the organism (11, 41, 58). Proapoptotic proteins Bax, Puma, Noxa, and Bid have been identified as p53 target genes (37, 40, 44, 55). An oligonucleotide array analysis revealed a number of p53 target genes that can be categorized as cell cycle arrest related (p21, GADD45, 14–3-3σ), apoptosis related (FAS, DR5), or oxidative stress related (superoxide dismutase, Pig 3) (71).

The stability of p53 is controlled by posttranslational modifications such as phosphorylation and acetylation. Multiple phosphorylation sites have been identified on the NH_2-terminal end of p53. However, the most well-studied phosphorylation site is Ser 15, which is known to be essential for the transactivation of p53. Phosphorylation of p53 could be mediated by DNA protein kinase (26, 66), ATM (2, 5), ATR (62), p38 (17, 57), p42/p44ERK (49, 69), p46/p54JNK (4, 36), Chk1 (59), and Chk2 (15).

Pifithrin-α (PFT-α) is a reversible inhibitor of p53 that has been shown to mediate antiapoptotic effects in several in vitro and in vivo systems (13). It was first reported by Komarov et al. (22) to block p53 transactivation and protect mice from the side effects of cancer therapy. Subsequently, Culmsee et al. (7) showed that PFT-α protected neurons from excitotoxic and ischemic insults by blocking Bax expression and mitochondrial dysfunction. Most recently, our study showed that PFT-α could protect cardiac functions in mice by inhibiting apoptosis (32).

The present study was designed to examine the consequences of p53 inhibition by PFT-α on Dox-induced apoptosis in rat embryonic myocardial H9c2 cells. These cells were chosen because they have been used to study the cellular mechanisms and pathways that are involved in oxidative stress and energy deprivation. They have also been used to study the mechanism of Dox-induced cardiotoxicity (27). We hypothesized that PFT-α can attenuate Dox-induced apoptosis by inhibiting p53 phosphorylation, thus preventing the activation of p53 downstream events such as caspase activation.

MATERIALS AND METHODS

Cell culture and materials. Rat embryonic ventricular myocardial H9c2 cells were obtained from American Type Culture Collection (Manassas, VA). Cells were cultured in DMEM (GIBCO, Invitrogen, Carlsbad, CA) containing 10% fetal bovine serum (FBS), 2 mM L-glutamine, and 25 μg/ml gentamicin at 37°C in a humidified atmosphere of 5% CO_2. Dox was purchased from Sigma Chemical (St. Louis, MO). Fetal bovine serum was obtained from Biosource

Address for reprint requests and other correspondence: C. C. Chua, Cardiovascular Research Laboratory, East Tennessee State Univ., Johnson City, TN 37614 (e-mail: chuac@etsu.edu).

The costs of publication of this article were defrayed in part by the payment of page charges. The article must therefore be hereby marked "*advertisement*" in accordance with 18 U.S.C. Section 1734 solely to indicate this fact.

International (Camarillo, CA). PFT-α, digitonin, SB-203580, PD-98059, and SP-600125 were products of Calbiochem (La Jolla, CA). Antibodies against phospho-site-specific p53 at Ser-15, active caspase-3, active caspase-9, poly(ADP ribose) polymerase (PARP), phospho-site-specific p42/p44ERK, total p38, total p42/p44ERK, and total p46/p54JNK were obtained from Cell Signaling Technology (Beverly, MA). Monoclonal caspase-8, caspase-2L, p53, Fas, phospho-site-specific p38, and phospho-site-specific p46/p54JNK antibodies were obtained from Santa Cruz Biotechnology (Santa Cruz, CA). Rat monoclonal caspase-12 antibodies were from Dr. Junying Yuan of Harvard Medical School. Mouse monoclonal cytochrome *c* and actin antibodies were purchased from Molecular Probes (Eugene, OR) and Sigma Chemical, respectively. Secondary antibodies were obtained from Jackson ImmunoResearch Laboratories (West Grove, PA).

Western blot analysis. Near confluent H9c2 cells (4×10^6) in 100-mm dishes were incubated with DMEM containing 0.5% FBS for 16 h so that the cells were semiquiescent. Dox was added directly to the conditioned medium at a final concentration of 5 μM for a designated period. In experiments that involved PFT-α, cells were pretreated with 20 μM PFT-α during the serum starvation period. Cells were harvested in a buffer containing 20 mM Tris·HCl (pH 7.8); 137 mM NaCl; 15% glycerol; 1% Triton X-100; 2 μg/ml each of leupeptin, aprotinin, and pepstatin; 2 mM benzamidine; 20 mM NaF; 10 mM sodium pyrophosphate; 1 mM sodium vanadate; 25 mM β-glycerophosphate; and 1 mM phenylmethylsulfonyl fluoride. Protein concentration was determined by Bio-Rad protein assay (Bio-Rad, Hercules, CA). Aliquots of 30 μg of lysates were electrophoresed on 12% SDS-PAGE and transferred to nitrocellulose membranes. Western blot analysis was carried out with primary antibodies at 4°C overnight. Appropriate secondary antibodies conjugated to horseradish peroxidase were then added for 1.5 h. Antigen-antibody complex was detected by using enhanced chemiluminescence reagent (Amersham Biosciences, Piscataway, NJ). Band density was measured by AlphaEase Image Analysis Software (Alpha Innotech, San Leandro, CA).

Caspase activity assays. H9c2 cells (4×10^6) in 100-mm dishes were treated with 5 μM Dox and/or 20 μM PFT-α for 16 h. Cells were scraped into ice-cold PBS, washed twice with PBS, and resuspended in a lysis buffer containing 50 mM HEPES, pH 7.4, 0.1% CHAPS, 0.1 mM EDTA, and 5 mM dithiothreitol (DTT). Protein concentration was determined by Bio-Rad protein assay. Caspase-2, -3, -8, and -9 activities were assayed using fluorogenic substrates (Ac-VDVAD-AMC for caspase-2, AcDEVD-AMC for caspase-3-like, AcIETD-AMC for caspase-8, and AcLEHD-AMC for caspase-9). Reaction mixture contained 70 μl of 1× reaction buffer (50 mM HEPES, pH 7.4, 100 mM NaCl, 0.1% CHAPS, 10 mM DTT, 1 mM EDTA, 10% glycerol), 20 μl of cell lysates (30 μg protein), and 10 μl of substrate (0.3 mM). Reaction was carried out at 37°C for 3 h. On cleavage of substrates by caspases, free AMC was read in a Tecan fluorescence plate reader (excitation 360 nm, emission 465 nm). Results were expressed as relative fluorescence units per microgram protein per hour.

Cytochrome c release. Cells (6×10^5) grown in 35-mm dishes were treated with Dox and/or PFT-α for 16 h. Mitochondria were isolated by the digitonin permeabilization method as described by Leist et al. (28). This method avoided the disruption of mitochondrial membrane by mechanical grinding. Digitonin is a weak nonionic detergent. At low concentrations, it can permeabilize plasma membrane and release cytosolic components from cells. Briefly, H9c2 cells were permeabilized with a buffer containing 210 mM mannitol, 70 mM sucrose, 10 mM HEPES, pH 7.8, 5 mM succinate, 0.2 mM EGTA, 0.15% BSA, and 80 μg/ml digitonin, on ice for 5 min. Cells were centrifuged at 12,000 *g* for 10 min, and 5 μg of the supernatant was separated on 12% SDS-PAGE. Western blotting was carried out with cytochrome *c* antibodies. A duplicate blot was probed with actin antibodies to check for protein loading.

Electrophoretic mobility shift assays. H9c2 cells (4×10^6) in DMEM containing 10% FBS were treated with or without 5 μM Dox and/or 20 μM PFT-α for 5 h. Nuclear extracts were prepared by a Nuclear Extraction kit (Active Motif, Carlsbad, CA), and protein concentration was determined by Bio-Rad dye-binding method. Synthetic consensus p53 binding sequence (Santa Cruz Biotechnology) was end-labeled with [γ-^{32}P]ATP by T4 polynucleotide kinase (Promega, Madison, WI). Binding reactions were carried out in a final volume of 10 μl containing 5 μg of nuclear extract, 10 mM HEPES, pH 7.9, 4 mM Tris·HCl, 60 mM KCl, 1 mM EDTA, 1 mM DTT, 10% glycerol, and ^{32}P-labeled probe. Reactions were incubated at room temperature for 30 min. DNA-protein complex was separated on a 5% polyacrylamide gel in 0.5× TBE (1× TBE: 0.045 M Tris-borate, 1 mM EDTA). Gel was dried and exposed to Kodak BioMax films. For supershift assays, 1 μg of anti-p53 antibody (clone Ab421, Oncogene Research Products, San Diego, CA) was included in the reaction.

Apoptosis assays. Quantitative analysis of apoptosis was performed with a Cell Death ELISA plus kit (Roche, Indianapolis, IN). Cells (5×10^4) were plated in 48-well dishes, changed to DMEM containing 0.5% FBS for 16 h, and treated with Dox and/or PFT-α for 7 h. Cells were lysed with 0.2 ml lysis buffer provided in the kit at room temperature for 20 min. Quantities of histone-associated DNA fragments (mononucleosomes and oligonucleosomes) were determined by absorbance at 405 nm with a Tecan microplate reader.

Statistical analysis. Statistical analyses were performed by one-way ANOVA followed by Tukey's multiple comparison test to show differences between means. Data were represented as means ± SE. $P < 0.05$ was considered significant.

RESULTS

To explore the effects of Dox on p53 levels, serum-starved H9c2 cells were treated with 5 μM Dox for different time periods. This concentration was chosen because it reproduces the plasma peak level achieved in patients receiving standard infusions of Dox (12). In our study, Dox triggered a time-dependent increase of p53 (Fig. 1*A*).

Because the stability of p53 is regulated by posttranslational modifications such as phosphorylation, and because phosphorylation of p53 at Ser15 is known to be essential for the transactivation of p53, we studied the effect of Dox on the level of phosphorylated p53 at Ser15. Western blot analysis was carried out with a specific antibody against phospho-p53 at

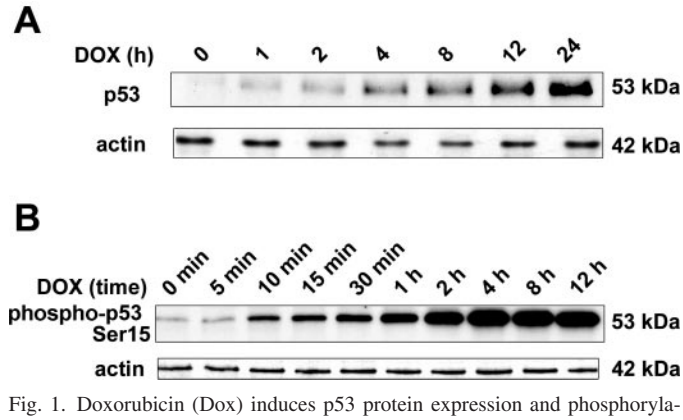

Fig. 1. Doxorubicin (Dox) induces p53 protein expression and phosphorylation of p53 at Ser15 in H9c2 cells. Cells were harvested after treatment with or without 5 μM Dox for the indicated periods. Thirty micrograms of total cell lysates were electrophoresed and probed with antibodies against p53 (*A*) or phospho-p53 (Ser15) (*B*). Duplicate blot was probed with actin antibodies to check for protein loading. Experiments were repeated 3 times, and representative data are shown.

Ser15. Figure 1*B* shows that Dox treatment led to a time-dependent increase of phospho-p53 at Ser15. Densitometric analysis demonstrated an increase of 3.3-fold and 4.7-fold after 30 min and 4 h of Dox treatment, respectively.

To determine whether MAP kinases (MAPKs) are affected by Dox administration, Western blot analysis was carried out with antibodies against phospho-site-specific MAPKs, including p38, p42/p44ERK, and p46/p54JNK. In addition, Western blot analysis was carried out with antibodies against total p38, p42/p44ERK, and p46/p54JNK. We found that Dox induced a transient increase in phosphorylation of all three MAPKs. Phosphorylation of p38 reached a peak 10 min after Dox treatment, after which phosphorylation returned to baseline. Pretreatment of H9c2 cells with 20 μM of a specific p38 inhibitor, SB-203580, completely blocked the elevation in phospho-p38 level (Fig. 2*A*). This concentration of SB-203580 was chosen according to the experimental design of a previous study (6).

Phosphorylation of p42/p44ERK and p46/p54JNK reached a peak 30 min after Dox treatment, after which phosphorylation returned to baseline. The elevation in p42/p44ERK and p46/p54JNK levels was abolished by 20 μM PD-98059 and 10 μM SP-600125, which are specific inhibitors of p42/p44ERK and p46/p54JNK, respectively (Fig. 2, *B* and *C*). The concentrations of these inhibitors were chosen according to the experimental design of previous studies (3, 47). These results indicated that Dox can transiently activate all three MAPKs. It is noted that 20 μM PD-98059 by itself induces the phosphorylation of p42/p44ERK. In addition, 10 μM SP-600125 seems to have a slight effect on JNK protein content.

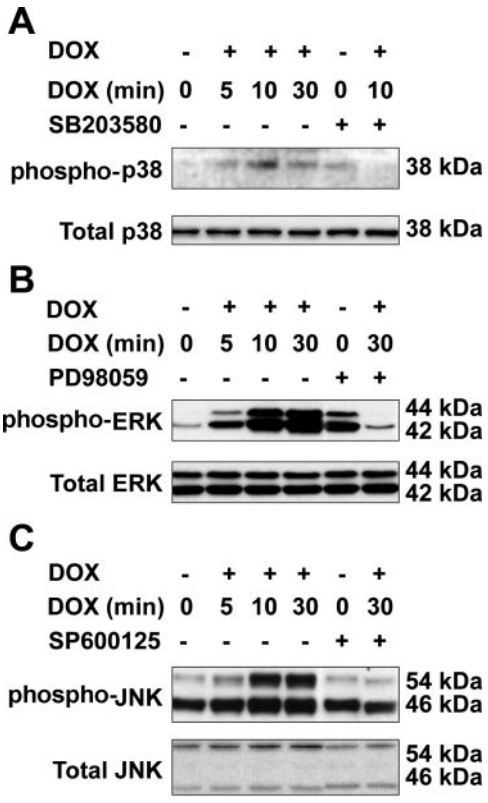

Fig. 2. Dox activates p38, p42/p44ERK, and p46/p54JNK MAPKs in H9c2 cells. Cells were pretreated 2 h with 20 μM SB-203580, 2 h with 20 μM PD-95059, or 10 min with 10 μM SP-600125 before treatment with 5 μM Dox for indicated periods and were harvested. Western blot analysis was carried out with phospho-specific antibodies against p38 (*A*), p42/p44ERK (*B*), or p46/p54JNK (*C*). Duplicate blot was probed with antibodies against total MAPKs.

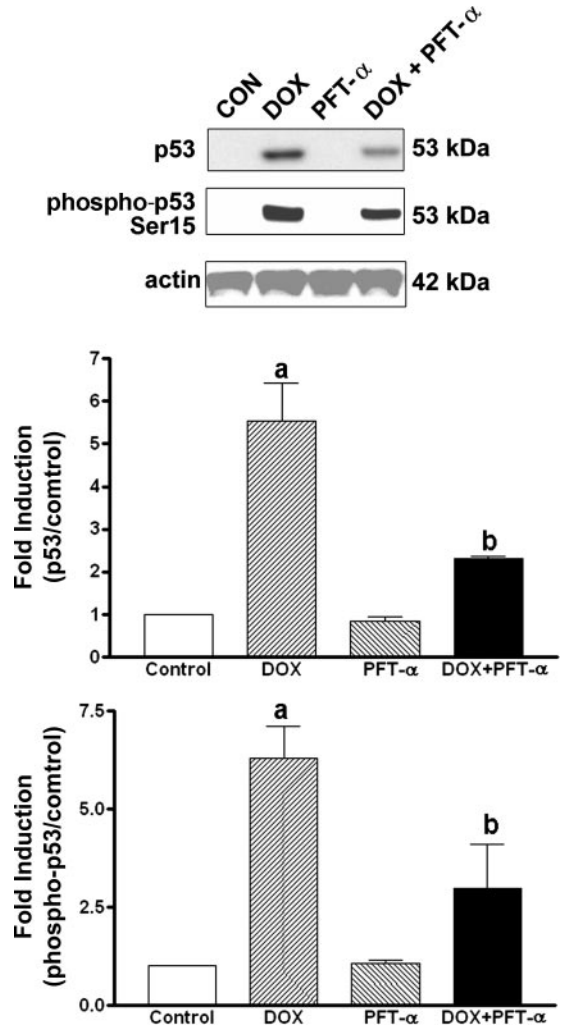

Fig. 3. Effect of pifithrin-α (PFT-α) and Dox on the expression of p53 and phospho-p53 (Ser15). H9c2 cells were treated with 5 μM of Dox and/or 20 μM PFT-α for 8 h. Western blot analysis was performed on 30-μg cell lysates with antibodies against p53 or phospho-p53 (Ser15). Actin was included to check for protein loading. Bar graph shows fold of induction of p53 and phospho-p53 (Ser15) after Dox and/or PFT-α treatment vs. control (Con) by image analysis. Data represent means ± SE from 4 samples. [a]$P < 0.05$, Dox-treated vs. control cells. [b]$P < 0.05$, Dox + PFT-α-treated cells vs. Dox-treated cells.

We next explored the effect of PFT-α, a chemical inhibitor of p53, on Dox-induced levels of p53 and phospho-p53. H9c2 cells were treated with Dox in the presence or absence of PFT-α for 8 h. The levels of p53 and phospho-p53 at Ser15 were determined by Western blot analysis. We found that Dox-induced upregulation of p53 and phospho-p53 (Ser15) could be attenuated by PFT-α (Fig. 3).

To identify which MAPK is affected by PFT-α, we treated H9c2 cells with Dox in the presence or absence of PFT-α for 10 min or 30 min. Densitometric analysis revealed that at 30 min of treatment, PFT-α partially blocked Dox-induced phosphorylation of p42/p44ERK and p46/p54JNK (Fig. 4). However, PFT-α had no effect on the phospho-p38 level (results not shown).

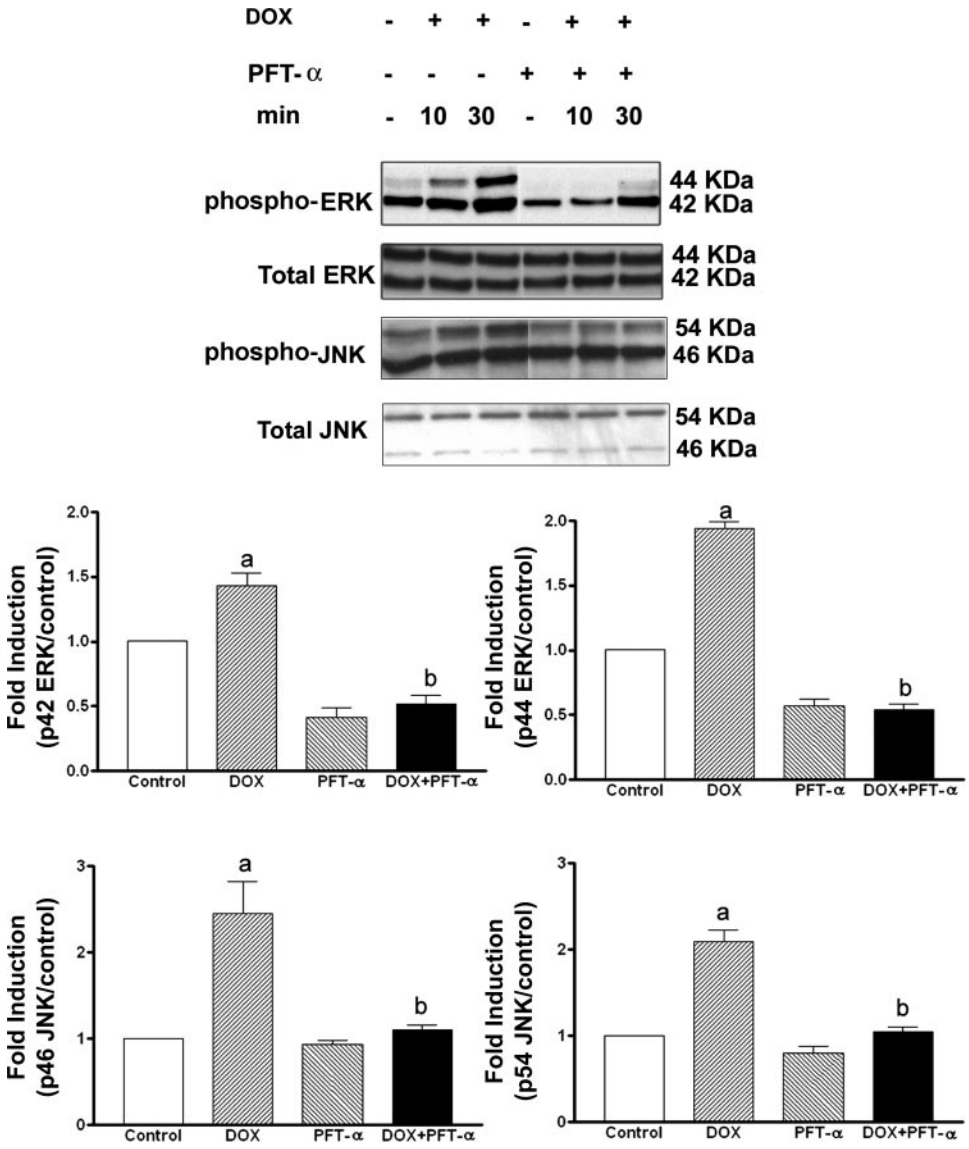

Fig. 4. Effect of PFT-α on p42/p44ERK and p46/p54JNK levels in Dox-treated cells. H9c2 cells were treated with 5 μM of Dox in the presence or absence of 20 μM PFT-α for designated times. Western blot analysis was carried out with p42/p44ERK and p46/p54JNK antibodies. Duplicate blot was probed with antibodies against total MAPKs. Bar graph shows fold of induction of p42/p44ERK and p46/p54JNK at 30 min of Dox treatment vs. control by image analysis. Results were normalized against total p42/p44ERK or total p46/p54JNK levels. Data represent means ± SE from 4 samples. [a]$P <$ 0.05, Dox-treated vs. control cells. [b]$P <$ 0.05, Dox + PFT-α-treated cells vs. Dox-treated cells.

Electrophoretic mobility shift assay showed that p53 binding activity was induced after Dox treatment for 5 h (Fig. 5, *lanes* 1 and *2*). PFT-α itself did not affect DNA binding activity of p53 (Fig. 5, *lane 3*). The addition of PFT-α attenuated Dox-induced p53 binding activity (Fig. 5, *lane 4*). In the presence of p53 antibody Ab421, a supershifted p53 complex was generated (Fig. 5, *lane 5*).

The effect of Dox on caspase activation was studied in H9c2 cells that were treated with Dox with or without PFT-α for 16 h. In these experiments, caspase-2, -3, -8, and -9 activities were measured by using specific fluorogenic substrates (Ac-VDVAD-AMC, Ac-DEVD-AMC, Ac-IETD-AMC, and Ac-LEHD-AMC). Results revealed that Dox activated caspases-2, -3, -8, and -9 by 3.77-, 2.1-, 2.2-, and 4.7-fold, respectively. The addition of PFT-α along with Dox partially suppressed these enzyme activities (Fig. 6, *A–D*). It is interesting to note that PFT-α by itself could significantly block the endogenous level of caspase-3 (Fig. 6*B*).

To investigate the expression of caspases and other apoptosis-related genes at the protein level, lysates were prepared from H9c2 cells treated with Dox and/or PFT-α for 8 h. This time point was chosen because there was some caspase activation in the control cells at 12 or 16 h as a result of low serum; this basal level of caspase activation would have interfered with the interpretation of any results derived from Dox-treated lysates prepared at 12 or 16 h. Western blot analysis was carried out with specific antibodies against caspases-2L, -3, -8, -9, -12, PARP, Fas, and actin. Caspases-2, -8, and -9 are initiator caspases (10, 38, 64) and caspase-3 is an executioner caspase (42), whereas caspase-12 is an endoplasmic reticulum (ER)-associated caspase (39). Activation of caspases-2L, -3, and -9 was detected with antibodies that recognize the 12-, 20-, and 17-kDa fragments of the respective active enzymes. Activation of caspases-2L, -3 and -9 was attenuated with the addition of PFT-α (Fig. 7). Procaspase-8 was barely detectable in untreated cells. After Dox treatment, there was an elevated level of 55-kDa procaspase and 44-kDa and 42-kDa activated fragments. The band density was decreased when PFT-α was added.

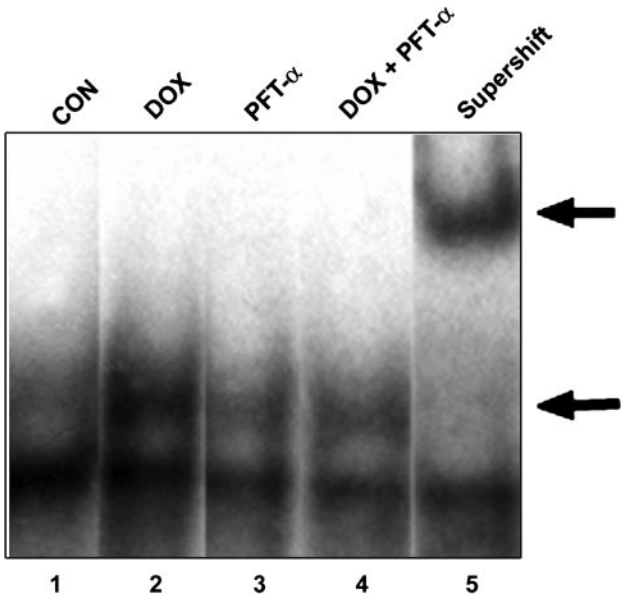

Fig. 5. p53 binding activity of H9c2 cells treated with Dox and/or PFT-α. Nuclear extracts were prepared from H9c2 cells stimulated with 5 μM of Dox for 5 h in the presence or absence of 20 μM of PFT-α. Electrophoretic mobility shift assay was performed as described in MATERIALS AND METHODS. Binding patterns of control (*lane 1*), Dox (*lane 2*), PFT-α (*lane 3*), Dox and PFT-α (*lane 4*), and Dox in the presence of p53 antibody Ab421 (*lane 5*) are shown. Bottom arrow indicates p53-DNA complex formation. Top arrow denotes supershifted complex in the presence of the p53 antibody Ab421. The experiment was conducted 4 times, and representative data are shown.

PARP is a substrate for caspase-3, and cleaved PARP has been shown to be an important marker for apoptosis (30). The pattern of PARP paralleled the pattern of active caspase-3. Caspase-12 was present as 60- and 54-kDa bands in untreated cells. On Dox treatment, the cleaved 54-kDa band was intensified. PFT-α could partially suppress the activation of caspase-12 (Fig. 7).

Fas is a cell surface protein that mediates apoptosis through a caspase-8-dependent pathway (67). Dox-upregulated FAS expression could be attenuated by PFT-α (Fig. 7).

Cytochrome *c* release is a marker for mitochondria-related apoptosis (29). H9c2 cells were permeabilized with 80 μg/ml of digitonin, and cytochrome *c* in the supernatant was subjected to Western blot analysis. Figure 8 shows that the release of cytochrome *c* was elevated after Dox treatment and that PFT-α partially blocked this elevation.

Quantification of apoptosis was performed by cell death ELISA assay. As shown in Fig. 9, Dox increased oligonucleosome formation by 1.8-fold. Cell death was inhibited by the addition of PFT-α along with Dox.

DISCUSSION

In this study, we present evidence that Dox rapidly upregulates p53, phosphorylated p53, p42/p44ERK, p38, and p46/p54JNK. We also demonstrate that Dox increases the activity of caspases-2, -3, -8, -9, and -12, leading to apoptosis. Most importantly, we demonstrate for the first time that PFT-α attenuates the apoptotic process by blocking Dox-induced expression of p53, phosphorylated p53, p42/p44ERK, p46/p54JNK, and the caspases listed above.

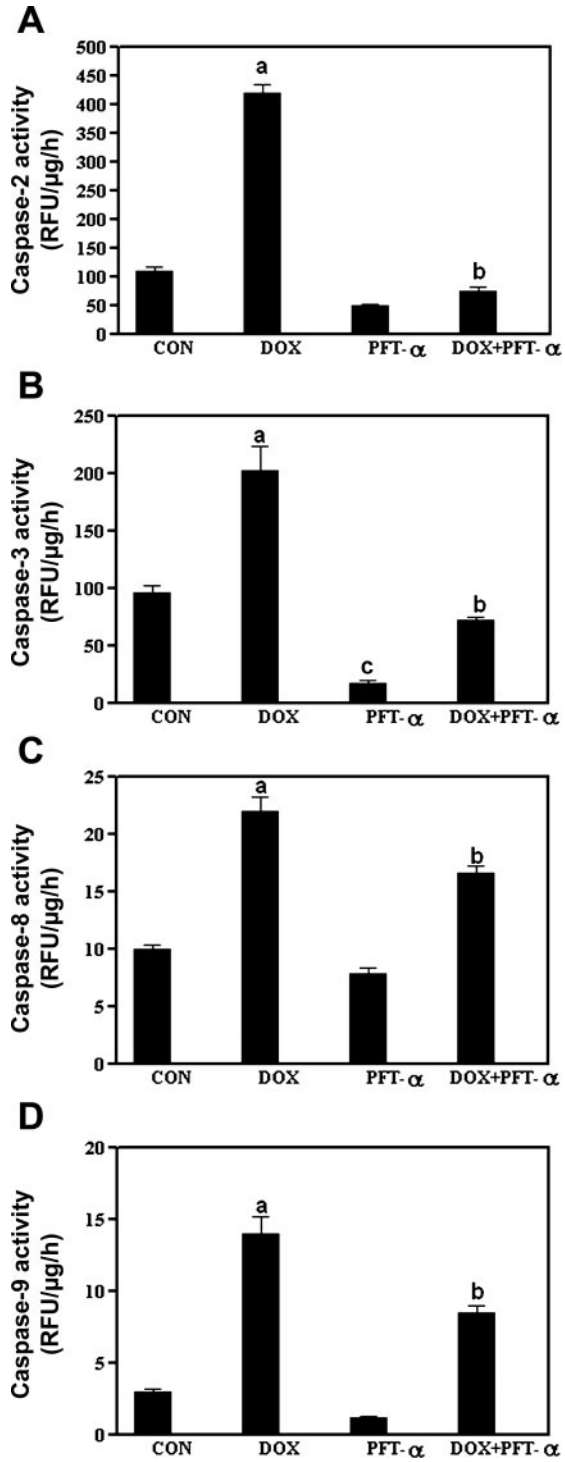

Fig. 6. Effect of Dox and PFT-α on caspase-2 (*A*), -3 (*B*), -8 (*C*), and -9 (*D*) activities in H9c2 cells. Caspase-2, -3, -8 , and -9 activities were measured in H9c2 cells treated with 5 μM of Dox in the presence or absence of 20 μM of PFT-α for 16 h by using specific fluorogenic substrates. Data represent means ± SE from 4 samples. $^{a}P < 0.05$, Dox-treated vs. control cells. $^{b}P < 0.05$, Dox + PFT-α-treated cells vs. Dox-treated cells. $^{c}P \leq 0.05$, PFT-α-treated cells vs. control cells. RFU, relative fluorescence units.

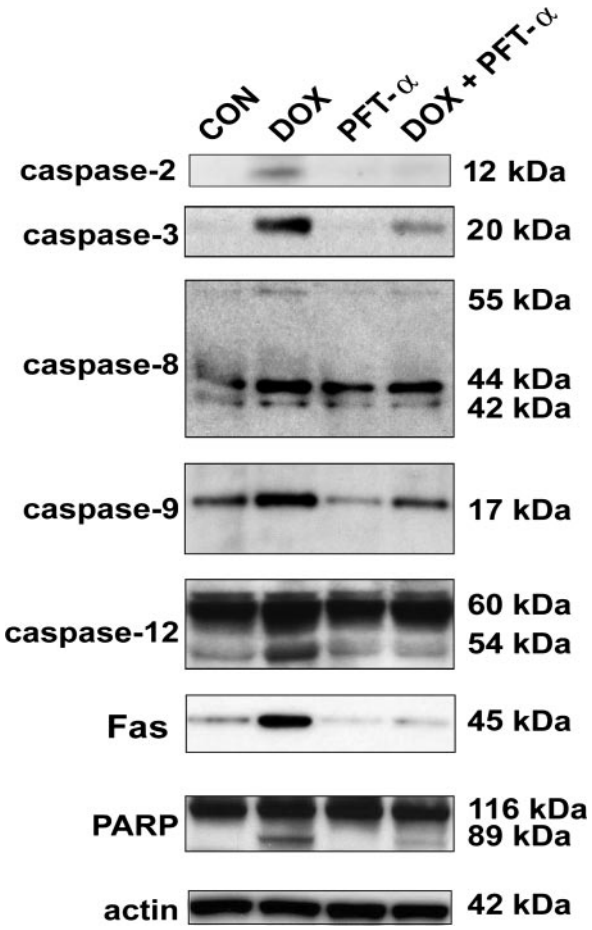

Fig. 7. Dox induces activation of caspases-2, -3, -8, -9, -12, poly(ADP ribose) polymerase (PARP), and Fas. H9c2 cells were treated with 5 μM of Dox and/or 20 μM of PFT-α for 8 h. Western blot analysis was carried out with antibodies against active caspase-2L, active caspase-3, caspase-8, active caspase-9, caspase-12, PARP, and Fas. Antibody against actin demonstrates equal loading of proteins. Experiments were repeated 3 times, and representative results are shown.

In our study, we found that Dox has an immediate effect on cell signaling pathways. Within 5–10 min, Dox rapidly phosphorylated all three MAPKs (Fig. 2). These results are in line with a study on the effect of daunomycin on the MAPKs in cardiomyocytes by Zhu et al. (72). In addition, we also found that Dox induced an upregulation of p53 level.

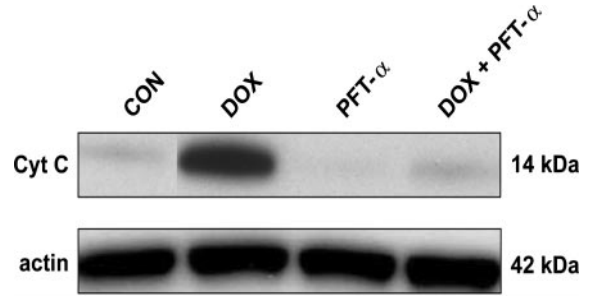

Fig. 8. Dox induces cytochrome *c* (Cyt *c*) release into the cytoplasm. H9c2 cells were treated with 5 μM of Dox and/or 20 μM PFT-α for 16 h. Digitonin was used to permeabilize plasma membrane. Cytochrome *c* released into the supernatant was analyzed by Western blot analysis. Actin was included as the protein loading control. Experiments were repeated 3 times, and representative results are shown.

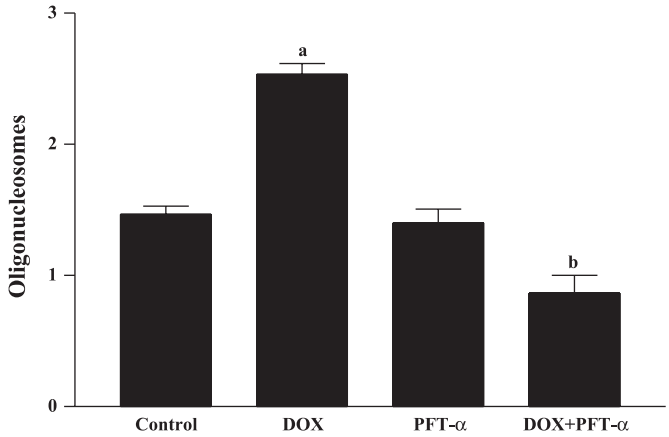

Fig. 9. Quantitative analysis of apoptosis. H9c2 cells in 48-well dishes were treated with 5 μM of Dox and/or 20 μM PFT-α for 16 h. Cell lysates were subjected to Cell Death ELISA assay. Oligonucleosomes were measured at 405 nm with the use of a microplate reader. Data represent means ± SE from 6 samples. $^{a}P < 0.05$, Dox-treated vs. control cells. $^{b}P < 0.05$, Dox + PFT-α-treated vs. Dox-treated cells.

Given that Dox triggered an increase in the proapoptotic p53, it is reasonable to assume that Dox has proapoptotic effects. In line with this hypothesis, our study showed that Dox induced a p53-dependent activation of caspases-2, -3, -8, -9, and -12 (Figs. 6 and 7) and triggered cytochrome *c* release (Fig. 8). This indicates that Dox induces both mitochondria-related and death receptor-related apoptotic pathways. Furthermore, in line with the results of Jang et al. (18), we also found that Dox activated caspase-12, indicating that Dox induces the ER-related apoptotic pathway. Caspase-12 resides in the ER and is activated on ER stress, including free radicals and disturbances of the intracellular calcium level (25, 39). Previous investigations have shown that Dox treatment leads to the generation of reactive oxygen species (27, 68) and an increase of calcium influx (24); this ER stress is hypothesized to activate caspase-12 and the ER-dependent apoptotic pathway. On activation, caspase-12 is translocated from the ER membrane to the cytosol where it may activate caspase-3 directly (52).

In our study, we also showed that Dox increased the level of caspase-2L (Figs. 6 and 7). Two isoforms of caspase-2 exist as a result of alternative splicing: caspase-2S and caspase-2L (9, 64). Recent studies indicate that these two proteins have opposite effects on apoptosis: caspase-2L induces apoptosis, whereas overexpression of caspase-2S is antiapoptotic. There is strong evidence that caspase-2L serves as a direct effector of the mitochondrial apoptotic pathway by releasing proapoptotic proteins, such as cytochrome *c*, or by cleaving Bid (14, 53).

Previous studies have demonstrated that p53 represses the expression of Bcl-2, PTEN (phosphatase and tensin homolog deleted on chromosome 10), and survivin and upregulates the gene expression of proapoptotic proteins such as Bax, Noxa, and Puma (50). Bax translocation induces cytochrome *c* release and allows the formation of apoptosomes, which contain caspase-9 and Apaf1. Caspase-9, in turn, activates caspase-3 and caspase-7, which execute the death program (35, 43).

A novel finding in our study is that PFT-α blocks the effects of Dox. First, Dox-induced elevation of p53 levels was partially blocked by PFT-α (Fig. 3). Previous studies have shown that PFT-α inhibits p53 accumulation in various cell systems

subjected to ultraviolet radiation, cisplatin, or resveratrol treatment (19, 22, 31, 70). To our knowledge, this is the first study that has shown that PFT-α can block Dox-induced p53 levels in H9c2 cells.

Second, we found that PFT-α was able to suppress Dox-induced apoptosis. Specifically, PFT-α partially blocked the induction of Dox-induced Fas in H9c2 cells (Fig. 7), a result that is in agreement with a previous study in human umbilical endothelial cells (33). In addition, PFT-α suppressed the activation of caspases-2, -3, -8, -9, and -12 (Figs. 6 and 7).

A reasonable question to ask is whether PFT-α blocks Dox-induced apoptosis through a p53-dependent mechanism, a p53-independent mechanism, or both. PFT-α has been reported to suppress other p53-independent effects. For example, Komarova et al. (23) found that PFT-α can suppress heat shock and glucocorticoid receptor signaling. In addition, PFT-α affects the transcription of a number of genes involved in DNA repair, apoptosis, and cell growth (48). In our study, PFT-α partially blocked the activation of p46/p54JNK and p42/p44ERK (Fig. 4), the activation of which are both p53 independent. Furthermore, in our study, PFT-α did not completely suppress the caspase activation and the overall apoptosis induced by Dox in H9c2 cells (Figs. 6 and 9), supporting the notion that there exists a p53-independent apoptotic pathway as described by Tsang et al. (63). It is possible that a p53-independent pathway plays an important part of the antiapoptotic effect of PFT-α, although this hypothesis needs to be explored further.

In summary, our results suggest that Dox induces apoptosis by upregulating p53 and caspases-2, -3, -8, -9, and -12 in H9c2 cells. We also present evidence that PFT-α partially attenuates these proapoptotic processes, although it is unclear whether the mechanism of this attenuation occurs through a p53-dependent pathway, a p53-independent pathway, or both. In our previous study, we demonstrated that PFT-α attenuated Dox-induced cardiac apoptosis in mouse hearts and had no effect on the tumor-killing activity of Dox in human prostate PC3 cells (32). As such, it is possible that combination therapy of PFT-α and Dox may be employed to prevent Dox-induced cardiotoxicity in patients who rely on Dox chemotherapy regimens.

ACKNOWLEDGMENTS

We thank Dr. Junying Yuan for caspase-12 antibodies.

GRANTS

This work was supported by Department of Veterans Affairs Merit Review and a Grant-in-Aid from the American Heart Association-Southeast Affiliate.

REFERENCES

1. **Arola OJ, Saraste A, Pulkki K, Kallajoki M, Parvinen M, and Voipio-Pulkki L.-M.** Acute doxorubicin cardiotoxicity involves cardiomyocyte apoptosis. *Cancer Res* 60: 1789–1792, 2000.
2. **Banin S, Moyal L, Shieh S, Taya Y, Anderson CW, Chessa L, Smorodinsky NI, Prives C, Reiss Y, Shiloh Y, and Ziv Y.** Enhanced phosphorylation of p53 by ATM in response to DNA damage. *Science* 281: 1674–1677, 1998.
3. **Bennett BL, Sasaki DT, Murray BW, O'Leary EC, Sakata ST, Xu W, Leisten JC, Motiwala A, Pierce S, Satoh S, Bhagwat SS, Manning AM, and Anderson DW.** SP600125, an anthra-pyrazolone inhibitor of Jun N-terminal kinase. *Proc Natl Acad Sci USA* 98:13681–13686, 2001.
4. **Buschmann T, Potapova O, Ivanov VN, Fuch SY, Henderson S, Fried VA, Minamoto T, Alarcon-Vargas D, Pincus MR, Gaarde WA, Holbrook NJ, Shiloh Y, and Ronai Z.** Jun NH_2-terminal kinase phosphorylation of p53 on Thr-81 is important for p53 stabilization and transcriptional activities in response to stress. *Mol Cell Biol* 21: 2743–2754, 2001.
5. **Canman CE, Lim DS, Cimprich KA, Taya Y, Tamai K, Sakaguchi K, Appella E, Kastan MB, and Siliciano JD.** Activation of the ATM kinase by ionizing radiation and phosphorylation of p53. *Science* 281: 1677–1679, 1998.
6. **Cuenda A, Rouse J, Doza YN, Meier R, Cohen P, Gallagher TF, Young PR, and Lee JC.** SB 203580 is a specific inhibitor of a MAP kinase homologue which is stimulated by cellular stresses and interleukin-1. *FEBS Lett* 364: 229–233, 1995.
7. **Culmsee C, Zhu X, Yu QS, Chan SL, Camandola S, Guo Z, Greig NH, and Mattson MP.** A synthetic inhibitor of p53 protects neurons against death induced by ischemic and excitoxic insults, and amyloid β-peptide. *J Neurochem* 77: 20–228, 2001.
8. **Delpy E, Hatem SN, Andrieu N, de Vaumas C, Henaff M, Rucker-Marti C, Jeffrezou JP, Laurent G, Levade T, and Mercadier JJ.** Doxorubicin induces slow ceramide accumulation and late apoptosis in cultured adult rat ventricular myocytes. *Cardiovasc Res* 43: 398–407, 1999.
9. **Droin N, Beauchemin M, Solary E, and Bertrand R.** Identification of caspase-2 isoform that behaves as an endogenous inhibitor of the caspase cascade. *Cancer Res* 60: 7039–7047, 2000.
10. **Duan H, Orth K, Chinnaiyan AM, Poirier GG, Froelich CJ, He WW, and Dixit VM.** ICE-LAP6, a novel member of the ICE/Ced-3 gene family, is activated by the cytotoxic T cell protease granzyme B. *J Biol Chem* 271: 16720–16724, 1996.
11. **Fridman JS and Lowe SW.** Control of apoptosis by p53. *Oncogene* 22: 9030–9040, 2003.
12. **Gianni L, Vigano L, Locatelli A, Capri G, Giani A, Tarenzi E, and Bonadonna G.** Human pharmacokinetic characterization and in vitro study of the interaction between doxorubicin and paclitaxel in patients with breast cancer. *J Clin Oncol* 15: 1906–1915, 1997.
13. **Gudkov AV and Komarova EA.** Prospective therapeutic applications of p53 inhibitors. *Biochem Biophys Res Commun* 331: 726–736, 2005.
14. **Guo Y, Srinivasula SM, Druilhe A, Fernandes-Alnemri T, and Alnemri ES.** Caspase-2 induces apoptosis by releasing proapoptotic proteins from mitochondria. *J Biol Chem 277*: 13430–13437, 2002.
15. **Hirao A, Kong YY, Matsuoka S, Wakeham A, Rudland J, Yoshida H, Liu D, Elledge SJ, and Mak TW.** DNA damage-induced activation of p53 by the checkpoint kinase Chk2. *Science* 287: 1824–1827, 2000.
16. **Hortobagyi GN.** Anthracyclines in the treatment of cancer. An overview. *Drugs* 54, *Suppl* 4: 1–7, 1997.
17. **Huang C, Ma WY, Maxiner A, Sun Y, and Dong Z.** p38 mediates UV-induced phosphorylation of p53 protein at serine 389. *J Biol Chem* 274: 12229–12235, 1999.
18. **Jang YM, Kendaiah S, Drew B, Phillips T, Selman C, Julian D, and Leeuwenburgh C.** Doxorubicin treatment in vivo activates caspase-12 mediated apoptosis in both male and female rats. *FEBS Lett* 577: 483–490, 2004.
19. **Jiang M, Yi X, Hsu S, Wang CY, and Dong Z.** Role of p53 in cisplatin-induced tubular cell apoptosis: dependence on p53 transcriptional activity. *Am J Physiol Renal Physiol* 287: F1140–F1147, 2004.
20. **Kang YJ, Zhou ZX, Wang GW, Buridi A, and Klein JB.** Suppression of metallothionein of doxorubicin-induced cardiomyocyte apoptosis through inhibition of p38 mitogen-activated protein kinases. *J Biol Chem* 275: 13690–13698, 2000.
21. **Keefe DL.** Anthracycline-induced cardiomyopathy. *Semin Oncol* 28: 2–7, 2001.
22. **Komarov PG, Komarova EA, Kondratov RV, Christov-Tselkov K, Coon JS, Chernov MV, and Gudkov AV.** A chemical inhibitor of p53 that protects mice from the side effects of cancer therapy. *Science* 285: 1733–1737, 1999.
23. **Komarova EA, Neznanov N, Komarov PG, and Gudkov A.** p53 inhibitor PFT-alpha can suppress heat shock and glucocorticoid signaling pathways. *J Biol Chem* 278: 15465–15468, 2003.
24. **Kusuoka H, Futaki S, Koretsune Y, Kitabatake A, Suga H, Kamada T, and Inoue M.** Alterations of intracellular calcium homeostasis and myocardial energetics in acute adriamycin-induced heart failure. *J Cardiovasc Pharmacol* 18: 437–444, 1991.
25. **Lamkanfi M, Kalai M, and Vandenabeele P.** Caspase-12: an overview. *Cell Death Differ* 11: 365–368, 2004.
26. **Lees-Miller SP, Sakaguchu K, Ullrich SJ, Appella E, and Anderson CW.** Human DNA-activated protein kinase phosphorylates serine 15 and 37 in the amino-terminal transactivation domain of human p53. *Mol Cell Biol* 12: 5041–5049, 1992.

27. **L'Ecuyer T, Allebban Z, Thomas R, and Vander Heide R.** Glutathione *S*-transferase overexpression protects against anthracycline-induced H9C2 cell death. *Am J Physiol Heart Circ Physiol* 286: H2057–H2064, 2004.
28. **Leist M, Volbracht C, Fava E, and Nicotera P.** Caspase-mediated apoptosis in neuronal excitoxicity triggered by nitric oxide. *Mol Pharmacol* 54: 789–801, 1998.
29. **Li P, Nijhawan D, Budihardjo I, Srinivasula SM, Ahmad M, Alnemri ES, and Wang X.** Cytochrome *c* and dATP-dependent formation of Afaf-1/caspase-9 complex initiates an apoptotic protease cascade. *Cell* 91: 479–489, 1997.
30. **Li X and Darzynkiewicz Z.** Cleavage of poly(ADP-ribose) polymerase measures in situ in individual cells: relationship to DNA fragmentation and cell cycle position during apoptosis. *Exp Cell Res* 255: 125–132, 2000.
31. **Lin HY, Shih A, Davis FB, Tang HY, Martino LJ, Bennett JA, and Davis PJ.** Resveratrol induced serine phosphorylation of p53 caused apoptosis in a mutant p53 prostate cancer cell line. *J Urol* 168: 748–755, 2002.
32. **Liu X, Chua CC, Gao J, Chen Z, Landy CL, Hamdy R, and Chua BH.** Pifithrin-α protects against doxorubicin-induced apoptosis and acute cardiotoxicity in mice. *Am J Physiol Heart Circ Physiol* 286: H933–H939, 2004.
33. **Lorenzo E, Ruiz-Ruiz C, Quesada AJ, Hernandez G, Rodriquez A, Lopez-Rivas A, and Redondo JM.** Doxorubicin induces apoptosis and CD95 gene expression in human primary endothelial cells through a p53-dependent mechanism. *J Biol Chem* 277: 10883–10892, 2002.
34. **Lown JW.** Anthracycline and anthraquinone anticancer agents: current status and recent developments. *Pharmacol Ther* 60: 185–214, 1993.
35. **Mihara M, Erster S, Zaika A, Petrenko O, Chittenden T, Pancoska p, and Moll UM.** p53 has a direct apoptogenic role at the mitochondria. *Cell* 11: 577–590, 2003.
36. **Milne DM, Campbell LE, Campbell DG, and Meek DW.** p53 phosphorylation in vitro and in vivo by an ultraviolet radiation-induced protein kinase characteristic of the c-Jun kinase, P46/P54JNK1. *J Biol Chem* 270: 5511–5518, 1995.
37. **Miyashita T and Reed J.** Tumor suppressor p53 is a direct transcriptional activator of the human bax gene. *Cell* 80: 293–299, 1995.
38. **Muzio M, Chinnaiyan AM, Kischkel FC, O'Rourke K, Shevshenko A, Ni J, Scaffidi C, Bretz JD, Zhang M, Gentz R, Mann M, Krammer PH, Peter ME, and Dixit VM.** FLICE, a novel FADD-homologous ICE/CED-3-like protease, is recruited to the CD95 (Fas/APO-1) death-inducing signaling complex. *Cell* 85: 817–827, 1996.
39. **Nakagawa T, Zhu H, Morishima N, Li E, Xu J, Yankner BA, and Yuan J.** Caspase-12 mediates endoplasmic-reticulum-specific apoptosis and cytotoxicity by amyloid-β. *Nature* 403: 98–103, 2000.
40. **Nakano K and Vousden KH.** PUMA, a novel proapoptotic gene, is induced by p53. *Mol Cell* 7: 683–694, 2001.
41. **Negoro S, Oh H, Tone E, Kunisada K, Fujio Y, Walsh K, Kishimoto T, and Yamauchi-Takihara K.** Glycoprotein 130 regulates cardiac myocyte survival in doxorubicin-induced apoptosis through phosphatidylinositol 3-kinase/Akt phosphorylation and Bcl-xL/caspase-3 interaction. *Circulation* 103: 555–561, 2001.
42. **Nicholson DW, Ali A, Thornberry NA, Vaillancourt JP, Ding CK, Gallant M, Gareau Y, Griffin PR, Labelle M, Lazebnik YA, Munday NA, Raju SM, Smulson ME, Yamin TT, Yu VL, and Miller DK.** Identification and inhibition of the ICE/CED-3 protease necessary for mammalian apoptosis. *Nature* 376: 37–43, 1995.
43. **Norbury CJ and Zhivotovsky B.** DNA damage-induced apoptosis. *Oncogene* 23: 2797–2808, 2004.
44. **Oda E, Ohki R, Murasawa H, Nemoto J, Shibue T, Yamashita T, Tokino T, Taniguchi T, and Tanaka N.** Noxa, a BH3-only member of the Bcl-2 family and candidate mediator of p53-induced apoptosis. *Science* 288: 1053–1058, 2000.
45. **Olson RD and Mushlin PS.** Doxorubicin cardiotoxicity: analysis of prevailing hypotheses. *FASEB J* 4: 3076–3086, 1990.
46. **Oren M.** Regulation of the p53 tumor suppressor protein. *J Biol Chem* 274: 36031–36034, 1999.
47. **Pang L, Sawada T, Decker SJ, and Saltiel AR.** Inhibition of MAP kinase kinase blocks the differentiation of PC-12 cells induced by nerve growth factor. *J Biol Chem* 270:13585–13588, 1995.
48. **Perfettini JL, Roumier T, Castedo M, Larocheette N, Boya P, Raynal B, Lazar V, Ciccosanti F, Nardacci R, Penninger J, Piacentini M, and Kroemer G.** NF-κB and p53 are the dominant apoptosis-inducing transcription factors elicited by the HIV-envelope. *J Exp Med* 199: 629–640, 2004.
49. **Persons DL, Yazlovitskaya EM, and Pelling JC.** Effect of extracellular signal-regulated kinase on p53 accumulation in response to cisplatin. *J Biol Chem* 275: 35778–35785, 2000.
50. **Philchenkov A.** Caspases: potential targets for regulating cell death. *J Cell Mol Med* 8: 432–444, 2004.
51. **Powis G.** Free radical formation by antitumor quinones. *Free Radic Biol Med* 6: 63–101, 1989.
52. **Rao RV, Castro-Obregon S, Frankowski H, Schuler M, Stoka V, del Rio G, Bredesen DE, and Ellerby HM.** Coupling endoplasmic reticulum stress to the cell death program. An Apaf-1-independent intrinsic pathway. *J Biol Chem* 277: 21836–21842, 2002.
53. **Robertson JD, Enoksson M, Suomela M, Zhivotovsky B, and Orrenius S.** Caspase-2 acts upstream of mitochondria to promote cytochrome *c* release during etoposide-induced apoptosis. *J Biol Chem* 277: 28903–28908, 2002.
54. **Sawyer DB, Fukazawa R, Arstall MA, and Kelly RA.** Daunorubicin-induced apoptosis in rat cardiac myocytes is inhibited by dexrazoxane. *Circ Res* 84: 257–265, 1999.
55. **Sax JK, Fei P, Murphy ME, Bernhard E, Korsmeyer SJ, and El-Deiry WS.** BID regulation by p53 contributes to chemosensitivity. *Nat Cell Biol* 4: 842–849, 2002.
56. **Seth R, Yang C, Kaushal V, Shah SV, and Kaushal GP.** p53-dependent caspase-2 activation in mitochondrial release of apoptosis-inducing factor and its role in renal tubular epithelial cell injury. *J Biol Chem* 280: 31230–31239, 2005.
57. **She Q, Chen N, and Dong Z.** p42/p44ERKs and p38 kinase phosphorylate p53 protein at serine 15 in response to UV radiation. *J Biol Chem* 275: 20444–20449, 2000.
58. **Sheikh MS and Fornace AJ Jr.** Role of p53 family members in apoptosis. *J Cell Physiol* 182: 171–181, 2000.
59. **Shieh SY, Ahn J, Tamai K, Taya Y, and Prives C.** The human homologs of checkpoint kinases Chk1 and Cds1 (Chk2) phosphorylate p53 at multiple DNA damage-inducible sites. *Genes Dev* 14: 289–300, 2000.
60. **Singal PK, Deally CM, and Weinberg LE.** Subcellular effects of adriamycin in the heart: a concise review. *J Mol Cell Cardiol* 19: 817–828, 1987.
61. **Singal PK and Iliskovic N.** Doxorubicin-induced cardiomyopathy. *N Engl J Med* 339: 900–905, 1998.
62. **Tibbetts RS, Brumbaugh KM, Williams JM, Sarkaria JN, Cliby WA, Shieh SY, Taya Y, Prives C, and Abraham RT.** A role for ATR in the DNA damage-induced phosphorylation of p53. *Genes Dev* 13: 152–157, 1999.
63. **Tsang WP, Chau SPY, Kong SK, Fung KP, and Kwok TT.** Reactive oxygen species mediate doxobubicin induced p53-independent apoptosis. *Life Sci* 73: 2047–2058, 2003.
64. **Wang L, Miura M, Bergerson L, Zhu H, and Yuan J.** Ich-1, an Ice/ced-3-related gene, encodes both positive and negative regulators of programmed cell death. *Cell* 78: 739–750, 1994.
65. **Wang L, Ma W, Markovich R, Chen JW, and Wang PH.** Regulation of cardiomyocyte apoptotic signaling by insulin-like growth factor I. *Circ Res* 83: 516–522, 1998.
66. **Wang Y and Eckhart W.** Phosphorylation sites in the amino-terminal region of mouse p53. *Proc Natl Acad Sci USA* 89: 4231–4235, 1992.
67. **Watanabe-Fukunaga R, Brannan CI, Itoh N, Yonehara S, Copeland NG, Jenkins NA, and Nagata S.** The cDNA structure, expression, and chromosomal assignment of the mouse Fas antigen. *J Immunol* 148: 1274–1279, 1992.
68. **Xu MF, Tang PL, Qian ZM, and Ashraf M.** Effects by doxorubicin on the myocardium are mediated by oxygen free radicals. *Life Sci* 68: 889–901, 2001.
69. **Yeh PY, Chuang SE, Yeh KH, Song YC, and Cheng AL.** Nuclear extracellular signal-regulated kinase 2 phophorylates p53 at Thr55 in response to doxorubicin. *Biochem Biophys Res Commun* 284: 880–886, 2001.
70. **Zhang M, Liu W, Ding D, and Salvi R.** Pifithrin-α suppresses p53 and protects cochlear and vestibular hair cells from cisplatin-induced apoptosis. *Neuroscience* 120: 191–205, 2003.
71. **Zhao R, Gish K, Murphy M, Yin Y, Notterman D, Hoffman WH, Tom E, Mack DH, and Levine AJ.** Analysis of p53-regulated gene expression patterns using oligonucleotide arrays. *Genes Dev* 14: 981–993, 2000.
72. **Zhu W, Zou Y, Aikawa R, Harada K, Kudoh S, Uozumi H, Hayashi D, Gu Y, Yamazaki T, Nagai R, Yazaki Y, and Komuro I.** MAPK superfamily plays an important role in daunomycin-induced apoptosis of cardiac myocytes. *Circulation* 100: 2100–2107, 1999.